

GISAXS and SAXS studies on the spatial structures of Co nanowire arrays^{*}

CHENG Wei-Dong(程伟东)^{1,2} MO Guang(默广)¹ XING Xue-Qing(邢雪青)^{1,2}
WANG De-Hong(王德红)^{1,2} GONG Yu(宫宇)^{1,2} CAI Quan(蔡泉)¹
CHEN Zhong-Jun(陈中军)¹ WU Zhong-Hua(吴忠华)^{1,1)}

¹ Institute of High Energy Physics, Chinese Academy of Sciences, Beijing 100049, China

² Graduate University of Chinese Academy of Sciences, Beijing 100049, China

Abstract: The spatial structures of magnetic Co nanowire array embedded in anodic aluminium membranes were investigated by grazing incidence small angle X-ray scattering (GISAXS) and conventional small angle X-ray scattering (SAXS) techniques. Compared with SEM observation, the GISAXS and SAXS measurements can get more overall structural information in a large-area scale. In this study, the two-dimensional GISAXS pattern was well reconstructed by using the IsGISAXS program. The results demonstrate that the hexagonal lattice formed by the Co nanowires is distorted ($a \approx 105$ nm, $b \approx 95$ nm). These Co nanowires are isolated into many structure domains with different orientations with a size of about 2 μm . The SAXS results have also confirmed that the nanopore structures in the AAM can be retained after depositing Co nanowires although the Co nanowires can not completely but only just fill up the nanopores. These results are helpful for understanding the global structure of the Co nanowire array.

Key words: grazing incidence small angle X-ray scattering, anode aluminum oxide, nanowire array

PACS: 61.05.cf, 62.23.Hj **DOI:** 10.1088/1674-1137/35/9/017

1 Introduction

In past decades, the rapid progress of the information industry has relied upon the development of magnetic storage materials and production technology. In order to acquire ultrahigh-density magnetic recording media, ferromagnetic nanomaterials have attracted wide attention. Especially, anodic alumina membrane (AAM) is often used to prepare a high-density metal nanowire array. This AAM-based metal nanowire array promises to have potential applications in electronic, photonic, magnetic and electrochemical devices. Recently, the ordered magnetic metal nanowire arrays, such as Fe, Ni, Co, Co-Cu and Co₃Pt, have been well prepared [1–5] by using the electrodeposition method. The magnetic measurements show that the perpendicular coercivity increases dramatically to a maximum at one temperature during the annealing process, but the paral-

lel coercivity does not have this phenomenon for the ordered Co-Cu, Co-Ag and Fe-Ag nanowire arrays, which can be attributed to the special anisotropic structures of these nanowires/AAM [1]. The magnetic properties of the Co nanowires array were found to be dominated by the polycrystalline particle shape and the interparticle magnetostatic interaction [3] and the reorientational transition of the anisotropy can be easily controlled by varying the aspect ratio. The research on the metastable Co-Cu solid solution nanowires demonstrates that the coercivity along the nanowire axis for the as-deposited samples increases, but it decreases for the annealed samples at 700 °C [5]. All this research shows the tight connection between the magnetic properties and the nanostructures. Synchrotron radiation techniques including EXAFS, XANES, SAXS and WAXS had been applied to detect the micro- and nanostructures of metallic nanowire array grown in aluminium oxide

Received 22 December 2010, Revised 13 February 2011

^{*} Supported by National Natural Science Foundation of China (10835008), Knowledge Innovation Program of Chinese Academy of Sciences (KJCX3-SYW-N8) and Momentous Equipment Program of Chinese Academy of Sciences (YZ200829)

1) E-mail: wuzh@ihep.ac.cn

©2011 Chinese Physical Society and the Institute of High Energy Physics of the Chinese Academy of Sciences and the Institute of Modern Physics of the Chinese Academy of Sciences and IOP Publishing Ltd

template. For example, in the highly-aligned parallel cylindrical Co nanowire array [6], the confined Co nanowires were found to contain a mixture of h.c.p. and f.c.c. phases in a ratio depending on the pore diameters in AAM. The crystallites of Fe or Co nanowires show that they strongly prefer orientation relative to the pore axis but are more isotropic in the case of Au and Ag. Small angle neutron scattering (SANS) [7] was also used to study the mesostructures for ordered anisotropic Co nanoparticles arrays formed in mesoporous aluminosilicate matrices with pore diameters of 2 nm. The results demonstrate the spatial correlation between magnetic and nuclear structure of ordered Co nanocomposites in mesoporous aluminosilicate. Grazing incidence small angle X-ray scattering (GISAXS) is a new technique, which is very sensitive to the surface morphology of the scattering entities either deposited on a flat substrate or buried in a thin layer [8–10]. Due to the small X-ray incidence angle and the limited penetration depth in the GISAXS geometry, the Born Approximation fails to describe correctly the scattering process. Thus, the Distorted Wave Born Approximation (DWBA) is frequently used [11]. This surface-sensitive GISAXS technique can give the in-plane and out-of-plane structural information of the sample. It is often used to probe the morphology of quantum dots or nanoparticles on or in the sample surface. For example, the drying process of a colloidal solution droplet of Co nanoparticles (10 nm diameter) on Si/Si₃N₄ substrates in magnetic field between 0.2 and 0.9 T was studied by GISAXS [12]. The results demonstrate that three dimensional rods of Co nanoparticles aligned perpendicularly to the substrate surface formed a hexagonally ordered pattern. Besides rods the labyrinthine structure can also be found at the border of the ordered rods area. Platschek et al. [13] also investigated the formation process and the subsequent transformation mechanism of mesostructured silica inside AAM by in situ GISAXS. In this paper, the GISAXS and SAXS techniques are used to study the Co nanowire array deposited in AAMs. Compared with the SEM observation, the GISAXS and SAXS techniques can provide the spatial structural information on a large area of the samples.

2 Experiments

The AAM with ordered nanochannels was prepared by a two-step anodizing process [14–16]. First, after annealing and electrochemically polishing, a

pure aluminium sheet was anodized at 10 °C, 0.3 M oxalic acid with an applied voltage of 40 V for 2 h. Subsequently, after removing the first-step alumina formed during the first step by using chemical etching, the sheet was further anodized for 10 h under the same condition. Then, after eliminating the aluminum and barrier layer at the bottom of AAM, a layer of Ag was sputtered onto one side of the membrane and was used as the working electrode in electro-deposition. Finally, the Co nanowire arrays were electrodeposited into the AAM using a direct current (1 V, 50 Hz) mode in 50 g/L CoSO₄ solution at room temperature.

GISAXS and SAXS measurements of the Co nanowires were carried out at Beamline 1W2A of Beijing Synchrotron Radiation Facility (BSRF) with wavelength of 0.154 nm. A Mar165 two-dimensional charge coupled device (CCD) detector with 2048×2048 pixels (each pixel 79 μm) was used to record the scattering patterns. The detector-to-sample distance was 5200 mm. For SAXS measurements, a transmission mode was used. In the GISAXS measurements, a lead strip was placed in front of the detector to stop the direct beam and the major reflection beam. The X-ray incidence angle was respectively set to 0.280°, 0.375°, 0.500° and 0.625°.

3 Results and discussion

The GISAXS patterns of Co nanowire array deposited in AAM are shown in Figs. 1(a)–(d) with these X-ray incidence angles of 0.280°, 0.375°, 0.500° and 0.625° respectively. In fact, different X-ray incidence angles represent different X-ray penetration depths. From Figs. 1(a)–(d), it can be seen that the GISAXS intensity decreases with the increasing of X-ray incidence angle. This change of GISAXS intensity demonstrates that the ordered degree of Co nanowire array decreases slightly with the depth increasing. A possible reason is that the pore diameter is not completely uniform in the whole length. With the increase of the penetration depth, the distribution width of the pore diameter in the AAM increases, resulting in the decrease of the GISAXS intensity. Another reason is that the X-ray path increases in the sample with the increase of X-ray incidence angle, which will lead to the increase of X-ray absorption and the decrease of scattering intensity.

The GISAXS intensities can be simply written as $I(q) = F(q)S(q)$, where \mathbf{q} is the scattering vector (momentum transfer, $\mathbf{q} = \mathbf{k}_f - \mathbf{k}_i$, $q = 4\pi \sin\theta/\lambda$, \mathbf{k}_f , \mathbf{k}_i are the incidence wave vector and scattering wave vector,

respectively). The form factor $F(q)$ depends on the shape and size of nanoparticles. The structure factor $S(q)$ relates to particle-particle correlation. On the GISAXS patterns, we take the horizontal direction as q_y direction, which corresponds to the in-plane scattering angles $2\theta_f$. And the vertical direction is the q_z direction related with the out-of-plane scattering angle α_f . Therefore, the change of GISAXS intensity with the scattering vector q_y is from the in-plane structure, while the change of GISAXS intensity with the scattering vector q_z is from the out-of-plane (i.e. the sample thickness direction) structure. From Figs. 1(a)–(d), it can be found that there are at least three obvious scattering peaks distributed respectively and symmetrically at two sides of the direction beam. It demonstrates that the Co nanowires have formed a long-range-order network in the sample plane.

In order to analyze further the lateral long-range-order structure in the sample plane, the GISAXS profile which changes with q_y is extracted at $q_z=0.21 \text{ nm}^{-1}$ as marked by the horizontal white-colour line in Fig. 1(a). Simultaneously, the GISAXS profile which changes with q_z is also extracted at $q_y=0.069 \text{ nm}^{-1}$ as marked by the vertical white-colour line. Both GISAXS profiles with the incidence angle of 0.280° are, respectively, shown in the top panel of Fig. 2 and its inset. Indeed, four scattering peaks can be easily distinguished and are, respectively, located at q_y values of 0.069, 0.120, 0.140 and 0.184 nm^{-1} . These q_y values have a proportional relation of 1: $3^{1/2}$: 2: $7^{1/2}$. This demonstrates that the Co nanowire array forms a hexagonal structure and the four peaks can be indexed as (100), (110), (200) and (210) reflections. We note that all the four peaks can be indexed as (hk0) reflections, which illustrates that the Co nanowire array forms a two-dimensional hexagonal structure in the sample plane. However, there is no periodic reduplication in the sample thick-

ness direction, which is confirmed by the q_z -direction GISAXS profile as shown in the inset of the top panel in Fig. 2, where only one GISAXS peak can be found. These GISAXS results are consistent with previous observation that the Co nanowires embedded in the AAM formed an in-plane hexagonal packed cylindrical arrangement [17, 18]. From these diffraction peaks of q_y direction, the average in-plane interplanar distance obtained is about 91.1 nm, the lattice parameter of hexagonal structure is about 105.2 nm. On the basis of GISAXS results, the in-plane Co nanowire density [19] can be evaluated with $\rho = d^{-2}$, here d is the average in-plane spacing of (100) crystal plane. For the Co nanowire array studied here, the density ρ_{GISAXS} obtained is $1.2 \times 10^{10} \text{ cm}^{-2}$. The GISAXS profiles with different X-ray incidence angles are compared in the bottom panel of Fig. 2. It can be seen that the GISAXS intensities decrease sharply, even the high-index diffraction peaks disappear gradually with the grazing angle increasing. However, it seems that the (100) reflection peak tends to split and shift to high- q value. This change indicates that the lattice parameter of the hexagonally ordered network of the Co nanowire array has a reduced tendency with the AAM depth increasing. The split of the (100) reflection implies the distortion of the hexagonal lattice. According to the separation positions of the (100) peak in the case of the X-ray incidence angle of 0.375° , the distortion of hexagonal unit cell can be evaluated with an oblique hexagonal lattice [20], and we get: $a=104.8 \text{ nm}$, $b=94.7 \text{ nm}$ and the angle γ between a and b axes is about 123.6° . The inset of Fig. 2 tells us that the decrease of GISAXS intensity with the increase of X-ray incidence angle is accompanied by the increase of the SAXS intensity. Evidently, with the decrease of the X-ray incidence angle, more incidence X-ray photons penetrate through the sample to cause more intense SAXS near the direct X-ray beam.

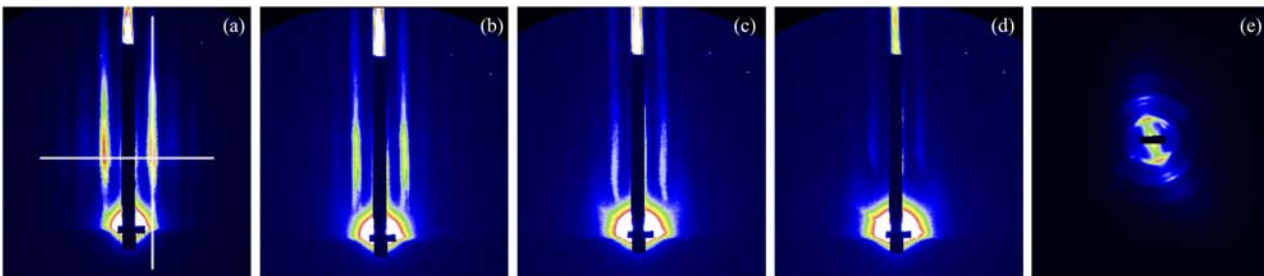


Fig. 1. The GISAXS patterns of the Co nanowires in AAM at an incidence angle of 0.280° (a), 0.375° (b), 0.500° (c) and 0.625° (d) respectively and the SAXS pattern of the AAM matrix filled with Co nanowire arrays (e).

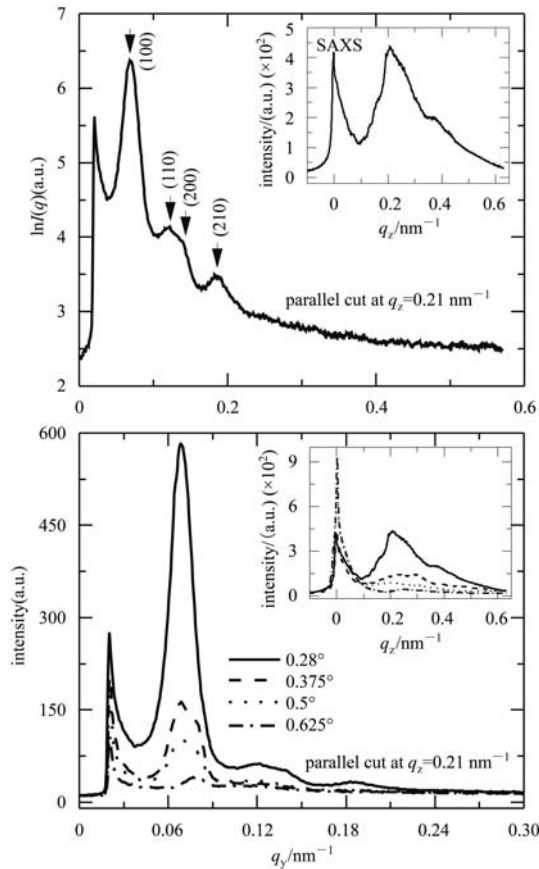


Fig. 2. Top panel: The GISAXS profiles of q_y -direction at $q_z=0.210 \text{ nm}^{-1}$ and q_z -direction at $q_y=0.069 \text{ nm}^{-1}$ (the insert) taken from the GISAXS pattern as marked by the white-colour lines in Fig. 1(a). The first extrema on the GISAXS profiles are from the SAXS intensity around the direct beam; Bottom panel: The GISAXS profile comparison of q_y -direction at $q_z=0.210 \text{ nm}^{-1}$ and q_z -direction at $q_y=0.069 \text{ nm}^{-1}$ (the insert) with X-ray incidence angles of 0.280° , 0.375° , 0.500° and 0.625° , respectively.

In order to have a better understanding of the global structures of the Co nanowire array, the two-dimensional GISAXS pattern of the Co nanowire array with X-ray incidence angle of 0.280° was simulated by using the IsGISAXS software [21–24]. A cylinder model was adopted in the calculation of the form factor. The DWBA formalism was used for this GISAXS simulation of Co nanowires buried in the AAM. The interference function was calculated based on a paracrystal model of hexagonal symmetry. First, the one-dimensional GISAXS profile along q_y -direction with $q_z=0.210 \text{ nm}^{-1}$ was quick-fitted with the Size-Spacing Correlation Approximation (SSCA) by using IsGISAXS program as shown in Fig. 3(a). The fitting parameters are obtained as follows: the cylinder radius is 19.7 nm , the aspect ratio of cylinder is 150 , the peak position of the interference function is 97.3 nm and the domain size is about 2000 nm . In the fitting, Gaussian functions were applied to describe the distributions of particle size, aspect ratio, interference function and lattice parameters. The experimental and simulated GISAXS patterns are compared in Figs. 3(b) and 3(c). It can be seen that all the experimental GISAXS features in Fig. 3(b), except the transmission SAXS signal around the direct beam, were well reconstructed in the simulated GISAXS pattern (Fig. 3(c)). In addition, the angle change between the regular hexagonal lattice orientation and the X-ray incidence beam has no influence on the simulative GISAXS pattern based on the quick-fit parameters. This illustrates that the Co nanowire array contains indeed plentiful structure domains with the size of about $2 \mu\text{m}$, but the relative orientations of these structure domains are not identical. The orientations of these structure domains inherit the orientations of aluminum grains in the aluminum sheet

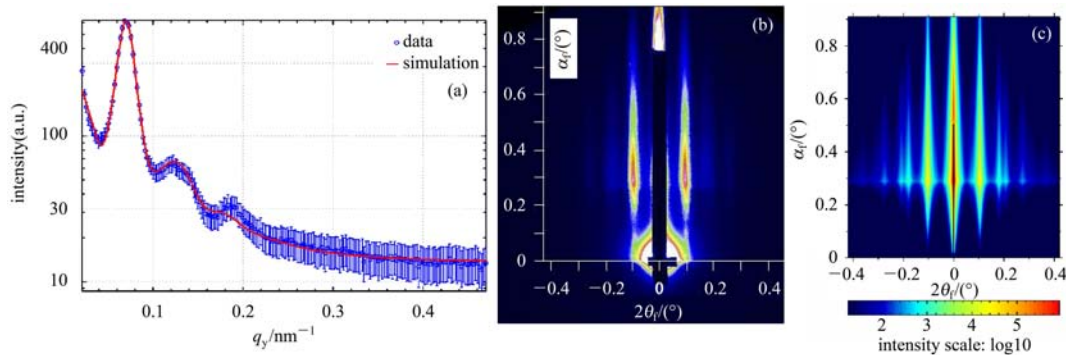


Fig. 3. Quick Fit (a) of the q_y -direction GISAXS profile at $q_z=0.210 \text{ nm}^{-1}$ by using IsGISAXS program, the circle line is the experimental value with error bar and the solid line is the simulation result; The experimental GISAXS pattern (b) of Co nanowire array in AAM with an incidence angle of 0.28° ; And the simulated GISAXS pattern (c) by using the IsGISAXS program with the parameters obtained in Quick Fit and the SEM results in Ref. [16].

used for AAM. Therefore, the GISAXS pattern of Co nanowire array should not be sensitive to the azimuth angle of the structure domain with hexagonal lattice. Therefore, we can conclude that the Co nanowire array resembles a polycrystalline arrangement in a large-area scale.

SAXS [25] has been widely used for investigating the size, shape and orientation of scatterers in the range of 1 to 200 nm. To verify the structural information of the Co nanowire array in AAM, SAXS measurements were also performed with the sample surface perpendicular to the X-ray incidence beam. Fig. 1(e) shows a preferential orientation in the SAXS pattern, which demonstrates that the ordered degree of the hexagonal lattice is anisotropic even within the sample area. One-dimensional SAXS curves of the AAM filled with or without Co nanowires are compared in Fig. 4. The SAXS intensities exhibit a sharp oscillation with at least six well-resolved diffraction peaks superimposed on a decay scattering background with q -value increase. The diffraction intensity of the AAM without Co nanowires is much higher than that with Co nanowires. This decrease of the diffraction peaks can be attributed to the increase of the structural disorder caused by the deposition of Co nanowires. In other words, the deposition of Co nanowires was not enough but just right for filling up the AAM nanopores. However, the same diffraction peak positions (0.069 , 0.120 , 0.140 , 0.180 and 0.210 nm^{-1}) in both cases with and without Co nanowires validate the retention of the original AAM structure. Based on the SAXS measurements, the largest interplanar distance obtained is about 92.6 nm and the lattice parameter is about 107 nm . These peaks can be, respectively, indexed as (100), (110), (200), (210) and (300) reflections with the hexagonal symmetry. These SAXS results are in good agreement with the GISAXS results.

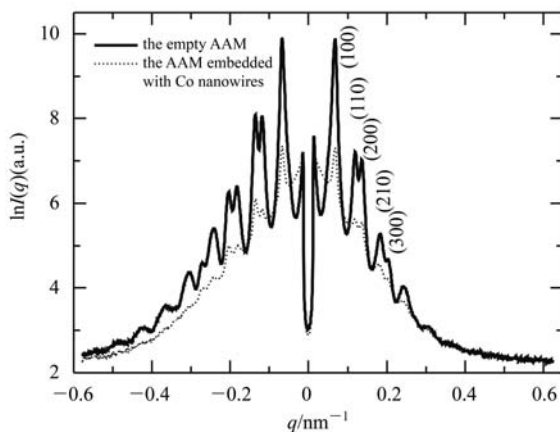


Fig. 4. The SAXS curves of the AAM filled with (dotted line) and without (solid line) Co nanowires.

4 Conclusion

The spatial structures of the Co nanowire array deposited in AAM were detected by using the GISAXS and SAXS techniques. A two-dimensional GISAXS pattern obtained from the experimental measurements was well reconstructed. The GISAXS results are consistent with the SAXS results. The following conclusions are obtained: In a large area scale, the cylindrical Co nanowires form hexagonal lattice in the sample plane with nanowire diameter of about 40 nm . But these Co nanowires are isolated into many structure domains with the size of about $2 \mu\text{m}$. The average hexagonal lattice of Co nanowires is slightly distorted ($a \approx 105 \text{ nm}$, $b \approx 95 \text{ nm}$) and has a preferential direction in the sample plane. Although the hexagonal structure of nanopores in the AAM can be retained after depositing Co nanowires, the Co nanowires are not sufficient but just right for filling up these nanopores. The density of nanowires in the sample area is about $1.2 \times 10^{10} \text{ cm}^{-2}$.

References

- 1 WANG Y W et al. J. Phys. Chem. B, 2002, **106**(10): 2502
- 2 Paulus P M et al. J. Magn. Magn. Mater., 2001, **224**(2): 180
- 3 SUN M et al. J. Phys. Lett., 2001, **78**(19): 2964
- 4 MIN J H et al. Phys. Stat. Sol. (a), 2007, **204**(12): 4158
- 5 WANG T et al. Phys. Stat. Sol. (a), 2006, **203**(10): 2426
- 6 Benfield R E et al. J. Alloys Comp., 2004, **362**(1-2): 48
- 7 Vyacheslavov A S et al. Mater. Sci. Eng. C, 2007, **27**(5-8): 1411
- 8 LIN Y et al. Nature, 2005, **434**: 55
- 9 Renaud G et al. Nucl. Instrum. Methods in Phys. Res. B, 2004, **222**(3-4): 667
- 10 Bernstorff S et al. Thin Solid Films, 2007, **515**(14): 5637
- 11 Sinha S K et al. Phys. Rev. B, 1988, **38**(4): 2297
- 12 Chushkin Y et al. Mater. Sci. Eng. C, 2006, **26**(5-7): 1136
- 13 Platschek B et al. Langmuir, 2008, **24**(9): 5018
- 14 LI G H et al. J. Phys.: Condens. Matter, 2003, **15**: 8663
- 15 BAI A et al. Electrochimica Acta, 2008, **53**(5): 2258
- 16 MO G et al. Appl. Phys. Lett., 2008, **93**(17): 171912
- 17 Fahmi A W et al. Macromol. Mater. Eng., 2006, **291**(9): 1061
- 18 Johnson B J S et al. Chem. Mater., 2004, **16**(15): 2909
- 19 Naudon A et al. Physica B, 2000, **283**(1-3): 69
- 20 Bondzic S et al. Polymer, 2008, **49**(11): 2669
- 21 Lazzari R. J. Appl. Crystallogr., 2002, **35**: 406
- 22 Lazzari R et al. Phys. Rev. B, 2007, **76**(12): 125411
- 23 Jedrecy N et al. Phys. Rev. B, 2005, **72**(4): 045430
- 24 Revenant C et al. Surf. Sci., 2007, **601**(16): 3431
- 25 MEN Y F et al. Macromolecules, 2004, **37**(25): 9481